Pseudonocardia abyssalis sp. nov. and *pseudonocardia oceani sp. nov*., two novel actinomycetes isolated from the deep Southern Ocean.

PARRA, J., SOLDATOU, S., ROONEY, L.M. and DUNCAN, K.R.

2021

INTERNATIONAL JOURNAL OF SYSTEMATIC AND EVOLUTIONARY MICROBIOLOGY

TAXONOMIC DESCRIPTION
Parra *et al.*, *Int. J. Syst. Evol. Microbiol.* 2021;71:005032
DOI 10.1099/ijsem.0.005032

MICROBIOLOGY SOCIETY
OPEN ACCESS

Pseudonocardia abyssalis sp. nov. and *Pseudonocardia oceani* sp. nov., two novel actinomycetes isolated from the deep Southern Ocean

Jonathan Parra, Sylvia Soldatou†, Liam M. Rooney‡ and Katherine R. Duncan*

Abstract

The actinomycetes strains KRD168^T and KRD185^T were isolated from sediments collected from the deep Southern Ocean and, in this work, they are described as representing two novel species of the genus *Pseudonocardia* through a polyphasic approach. Despite sharing >99% 16S rRNA gene sequence similarity with other members of the genus, comparative genomic analysis allowed species delimitation based on average nucleotide identity and digital DNA–DNA hybridization. The KRD168^T genome is characterized by a size of 6.31 Mbp and a G+C content of 73.44 mol%, while the KRD185^T genome has a size of 6.82 Mbp and a G+C content of 73.98 mol%. Both strains contain *meso*-diaminopimelic acid as the diagnostic diamino acid, glucose as the major whole-cell sugar, MK-8(H_4) as a major menaquinone and *iso*-branched hexadecanoic acid as a major fatty acid. Biochemical and fatty acid analyses also revealed differences between these strains and their phylogenetic neighbours, supporting their status as distinct species. The names *Pseudonocardia abyssalis* sp. nov. (type strain KRD168^T=DSM 111918^T=NCIMB 15270^T) and *Pseudonocardia oceani* (type strain KRD185^T=DSM 111919^T=NCIMB 15269^T) are proposed.

The genus *Pseudonocardia* was described for the first time by Hassen [1] and the description was subsequently amended [2–5]. Members of the genus *Pseudonocardia* are aerobic, Gram-positive, non-motile, catalase-positive bacteria. Typically, strains form branched substrate hyphae that may fragment into rod-shaped elements. Aerial hyphae, if formed, can be sterile, may be fragmented into chains of oval or square elements, or may differentiate into chains of spores. Substrate and aerial hyphae show cell division in different directions with a tendency to form swellings. Spores are usually smooth and may be formed on the substrate or aerial hyphae. The major menaquinone is MK-8(H_4) and the predominant fatty acid is *iso*-branched hexadecanoic acid, while mycolic acids are absent [6].

According to the List of Prokaryotic names with Standing in Nomenclature (LPSN), at the time of writing 63 species have been described for the genus *Pseudonocardia* with validly published names [7, 8]. In particular, this genus has been reported as including actinomycetes commonly isolated from marine sediments [9, 10]. Thus, a few species have been described from marine environments such as mangrove forest [11], coastal [12], bathyal [13], abyssal [14] and hadal [15] sediments.

In a preceding study, strains KRD168^T and KRD185^T were isolated from sediments collected in the deep Southern Ocean, showing potential as producers of antimicrobial metabolites [16, 17]. Therefore, this work aims to describe them as representing two novel species, *Pseudonocardia abyssalis* sp. nov. and *Pseudonocardia oceani* sp. nov.

ISOLATION AND ECOLOGY

The isolation of strains KRD168^T and KRD185^T was reported previously by Millán-Aguiñaga *et al.* [16]. Briefly, marine

Author affiliations: [1]Strathclyde Institute of Pharmacy and Biomedical Sciences, University of Strathclyde,, Glasgow G4 0RE, UK.
***Correspondence:** Katherine R. Duncan, katherine.duncan@strath.ac.uk
Keywords: Actinobacteria; ocean; *Pseudonocardia*; sediments.
Abbreviations: ANI, average nucleotide identity; autoMLST, automated multi-locus species tree; dDDH, digital DNA–DNA hybridization; ISP, International *Streptomyces* Project.
†Present address: School of Pharmacy and Life Sciences, Robert Gordon University, Aberdeen AB10 7GJ, UK
‡Present address: Institute of Biological Chemistry, Biophysics and Bioengineering, School of Engineering and Physical Sciences, Heriot-Watt University, Edinburgh EH14 4AS, UK.
The Whole Genome Sequencing project has been deposited at NCIB under BioProject PRJNA678748. The Whole Genome Shotgun project has been deposited at DDBJ/ENA/GenBank under accessions JADQDK000000000 and JADQDF000000000. The versions described in this paper are JADQDK010000000 and JADQDF010000000. The GenBank accession number for the 16S rRNA gene sequences are MH725312 and MH725295
Four supplementary tables and three supplementary figures are available with the online version of this article.
005032

sediment cores were obtained by the PS *Polarstern* (2002) during the ANDEEP II expedition. KRD168^T was isolated from dark greenish-grey silty clay collected in the North Weddell Kosminski Fracture Zone (62° 57.56′ S 27° 53.23′ W) at a depth of 4539 m, while KRD185^T was isolated from greenish-grey silty clay collected in the Weddell Abyssal Plain (65° 19.88′ S 48° 5.58′ W) at a depth of 4060 m [18]. The strains were isolated on artificial seawater agar (SW; Instant Ocean sea salt 18 g l^{-1}, agar 14 g l^{-1}) using the stamping method [19]. The strains were routinely cultured on ISP2 agar [20] supplemented with artificial seawater (18 g l^{-1}) and stored at −80 °C as glycerol suspensions (20%).

16S rRNA GENE PHYLOGENY

The almost-complete 16S rRNA gene sequences of strains KRD168^T and KRD185^T were obtained by PCR amplification using the 3-IDT (Integrated DNA Technology) primers FC27 (5′-AGAGTTTGATCCTGGCTCAG-3′) and RC1492 (5′-TACGGCTACCTTGTTACGACTT-3′) [21]. Sequences were compared to those within the National Center for Biotechnology Information (NCBI) database using the Basic Local Alignment Search Tool (BLAST) [22], and EzBioCloud [23]. A multiple alignment of all the sequences was achieved by using CLUSTAL X 2.1 [24], and their evolutionary relationships were assessed using neighbour-joining tree [25] reconstructions based on the Tamura–Nei model [26] using MEGA X [27] with 1000 bootstrap replications [28]. The nearly complete (93.1%) 16S rRNA gene sequence of strain KRD168^T was found to be closely related to *Pseudonocardia petroleophila* ATCC 15777^T (99.6%), *Pseudonocardia hydrocarbonoxydans* NRRL B-16171^T (99.4%) and *Pseudonocardia seranimata* YIM 63233^T (99.3%). Similarly, the nearly complete (95.0%) 16S rRNA gene sequence of strain KRD185^T was closely related to *Pseudonocardia broussonetiae* Gen01^T (99.6%), *P. petroleophila* ATCC 15777^T (98.9%), *P. hydrocarbonoxydans* NRRL B-16171^T (98.4%) and *P. seranimata* YIM 63233^T (98.4%). The neighbour-joining phylogenetic tree (Fig. 1) showed that both isolates formed a monophyletic group with *P. petroleophila* ATCC 15777^T, *P. seranimata* YIM 63233^T and *P. broussonetiae* Gen01^T. In particular, strain KRD168^T, *P. seranimata* YIM 63233^T and *P. petroleophila* ATCC 15777^T were part of the same branch, while strain KRD185^T and *P. broussonetiae* Gen01^T formed a second branch. This topology was also supported by the maximum-likelihood and maximum-parsimony trees (Fig. S1, available in the online version of this article).

GENOME FEATURES

A modified organic DNA extraction protocol [29] was performed for DNA isolation from strains KRD168^T and KRD185^T. Genomic DNA was sequenced at MicrobesNG for short-read sequencing. Genomic DNA libraries were prepared using a Nextera XT Library Prep Kit and sequenced on the Illumina HiSeq platform. Genomic DNA was also sequenced at NU-OMICS using PacBio technology for long-read sequencing. The polymerase binding reaction to SMRTbell template was performed using the Sequel Binding kit 2.1 and sequenced using a PacBio Sequel instrument with a 10 h movie capture time. Next, the BAM files of circular consensus sequencing reads were used for assembly in HGAP (v.4).

For strain KRD168^T, long reads were assembled using Flye [30] (v.2.8.1). Then, the short reads were mapped over the assembly using Bowtie2 [31] (v.2.4.2), and the produced BAM files were used for improving the genome using Pilon [32] (v.1.23) by correcting bases, fixing misassemblies and filling gaps. As a result, a complete genome sequence was obtained with 1150.6× genome coverage, comprising a chromosome sequence of 6273229 bp and a plasmid of 32760 bp, and with a G+C content of 73.44 mol%. For strain KRD185^T, a consensus assembly was created to reduce the number of contigs. To this end, long reads were first assembled using HGAP [33] (v.4), Flye (v.2.8.1), Canu [34] (v.2.1.1) and Raven [35] (v.1.2.2). Then, a consensus assembly was obtained with Flye using the 'subassemblies' mode. Finally, the consensus long-read assembly was integrated within Unicycler [36] (v.0.4.8), with SPAdes [37] (v.3.14.1) and Pilon (v.1.23) as dependencies, to create a hybrid assembly including short-read data. As a result of this strategy, an assembly made up of a chromosome of 6661555 bp, and presumably two plasmids of 99100 and 61150 bp, was obtained. The genome coverage for strain KRD185^T was 217.1×, and the G+C content was 73.98 mol%. Finally, the quality of both assemblies was evaluated using QUAST [38] (v.5.0.2), while their completeness was evaluated using BUSCO [39] (v.3.0.2) (Table S1).

To assess the genomic distance between strains KRD168^T and KRD185^T and other publicly available *Pseudonocardia* genomes (Table S2), digital DNA–DNA hybridization (dDDH) values were calculated with the Genome-to-Genome Distance Calculator (GGDC) [40] (v.2.1) using formula 2, while pairwise whole-genome average nucleotide identity (ANI) values were calculated using FastANI [41] (v.1.3). The calculated values (Fig. 2) showed that strain KRD168^T and *P. petroleophila* CGMCC 4.1532^T had a dDDH of 43.5% and an ANI of 91.8%, whilst strain KRD185^T and *P. broussonetiae* Gen01^T showed dDDH and ANI values of 51.7% and 93.7%, respectively. In both cases, the ANI values were below the recommended inter-species boundary value of 95% [41, 42]. Furthermore, the dDDH values also support the inter-species delimitation as they were below the threshold value of 70% [43]. Hence, despite the high sequence similarity (>99.5%) observed in the 16S rRNA gene between strain KRD168^T and *P. petroleophila* ATCC 15777^T, and between strain KRD185^T and *P. broussonetiae* Gen01^T, the whole-genome sequence relatedness indicated that strains KRD168^T and KRD185^T represent two novel species.

A genome-scale phylogenetic tree (Fig. 2) based on multilocus sequence analysis was reconstructed using autoMLST [44]. The list of used protein-coding genes can be found in Table S3. This analysis confirmed the evolutionary relationship between strains KRD168^T and KRD185^T, *P. petroleophila* CGMCC 4.1532^T and *P. broussonetiae* Gen01^T. Moreover, it

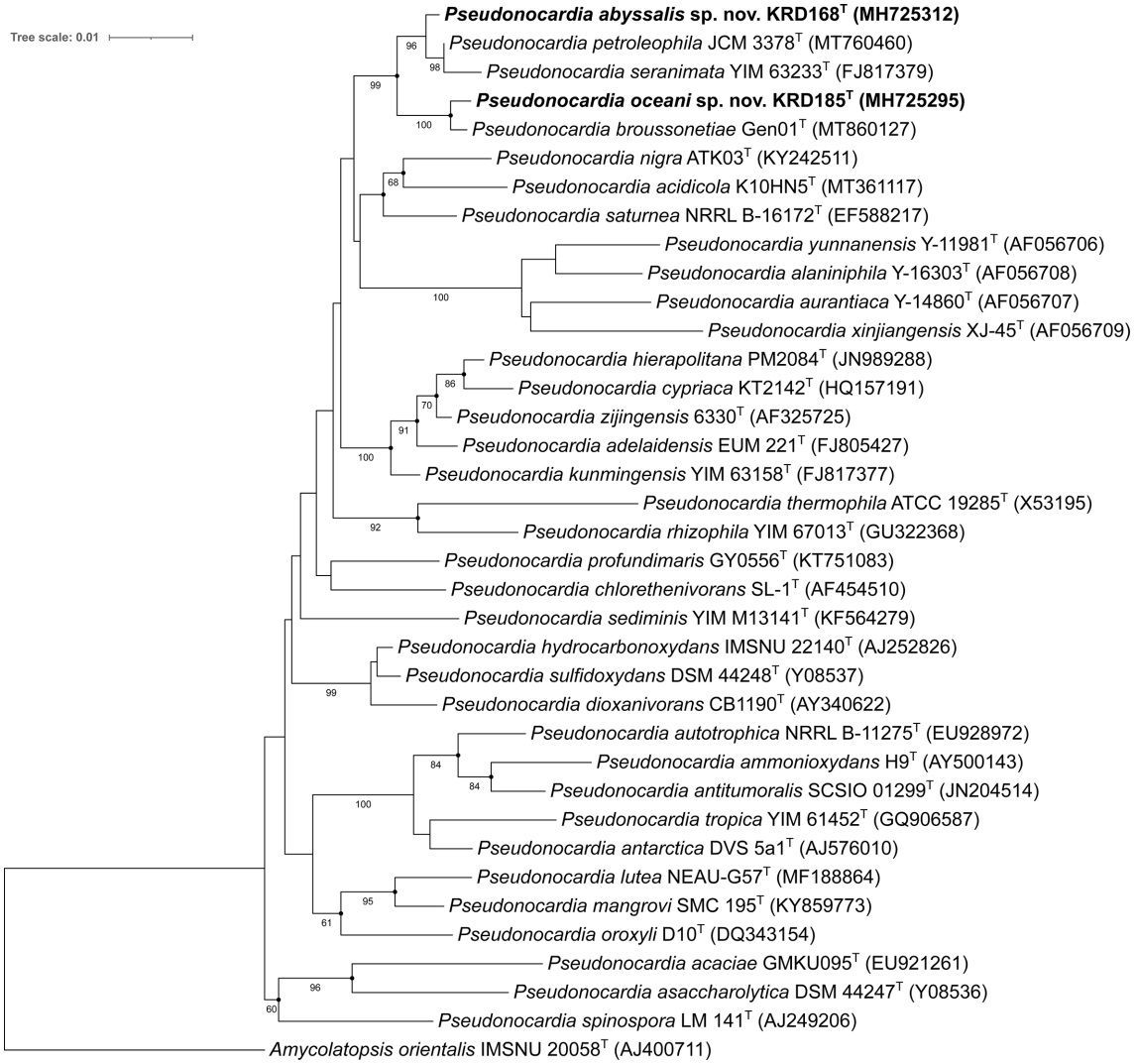

Fig. 1. Neighbour-joining phylogenetic tree based on 16S rRNA gene sequences showing the phylogenetic relationships of strains KRD168^T and KRD185^T and representative members of the genus *Pseudonocardia*. Dots on branches indicate those also recovered in the maximum-likelihood and maximum-parsimony trees. Bootstrap values of >50% are shown at branch points. *Amycolatopsis orientalis* IMSNU 20058^T was used as an outgroup. Bar, 0.01 substitutions per nucleotide position.

suggested a recent common ancestor between this monophyletic group and *Pseudonocardia thermophila* DMS 43832^T [1]. Interestingly, although the 16S rRNA gene phylogeny suggested a more distant relationship, the whole-genome analysis showed that *P. hydrocarbonoxydans* NBRC 14498^T [45] is closely related to strains KRD168^T and KRD185^T.

PHYSIOLOGY AND CHEMOTAXONOMY

The colony morphology of strains KRD168^T and KRD185^T, as well as *P. petroleophila* DSM 43193^T and *P. hydrocarbonoxydans* DSM 43281^T, was examined when cultured on ISP2, ISP3, ISP4 and ISP5 media [20] (Fig. S2). Salinity and pH tolerance analysis of the strains was carried out on modified ISP2 and ISP5 at pH 4–10 (Table S4) and with 0–20% (w/v) NaCl. The strains were able to grow on all tested media with no diffusible pigments produced. Despite their marine origin, strains KRD168^T and KRD185^T did not display a particularly high halotolerance in comparison with their closest relatives as they both grew well at an NaCl concentration of 3%, which was 1% less than *P. petroleophila* DSM 43193^T and 1% more than *P. hydrocarbonoxydans* DSM 43281^T (Table 1). Moreover, salt was not a requirement for growth.

Analyses of fatty acids, metabolic activity, respiratory quinones, polar lipids and whole-cell sugars were carried out by the Identification Service of the Leibniz Institute DSMZ – German Collection of Microorganisms and Cell Cultures. For these analyses, strains were cultivated in GYM medium (28 °C for 8–14 days). Fatty acid analysis was performed using the Sherlock MIS (MIDI) system after conversion into fatty acid methyl esters [46, 47]. The fatty

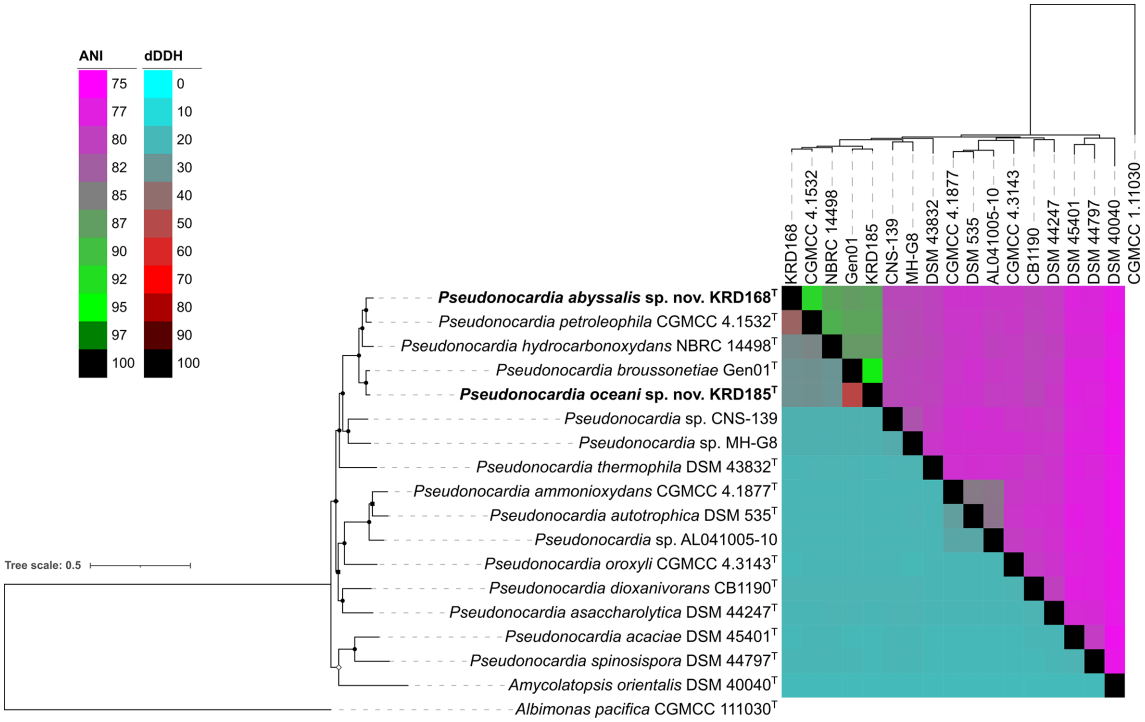

Fig. 2. Heatmap of the genomic distance between strains KRD168^T and KRD185^T and other *Pseudonocardia* strains, calculated as pairwise digital DNA–DNA hybridization (dDDH) (cyan, 0%; red, 70%) and average nucleotide identity (ANI) (magenta, 75%; green, 95%) values. The multi-locus tree based on 93 gene sequences extracted from the whole-genome sequence is shown. *Albimonas pacifica* CGMCC 111030^T was used as an outgroup. Bootstrap support is indicated as symbols in the branches (●=100, ◆=99, ■=98, ◇=95). Bar, 0.5 substitutions per nucleotide position.

acid annotations and quantification were made by the MIS Standard Software (Microbial ID) using the Aerobic Bacteria Library (TSBA6 v6.10). Metabolic activity was determined using the API 20E and API ZYM systems (bioMérieux). Polar lipids and respiratory quinones were extracted from freeze-dried cells cultured in YEME broth and analysed by chromatography [48]. Analysis of whole-cell sugars and detection of isomers of 2,6-diaminopimelic acid (Dpm) and 2,6-diamino-3-hydroxypimelic acid (OH-Dpm) were performed by TLC [49, 50].

The observed morphology of strains KRD168^T and KRD185^T, as well as the presence of *meso*-diaminopimelic acid in the cell-wall, MK-8(H_4) as the major menaquinone and *iso*-branched hexadecanoic acid as a predominant fatty acid, confirmed the typical physiology of a *Pseudonocardia* species for both strains. The polar lipid profile (Fig. S3) of both strains was characterized by the presence of phosphatidylethanolamine and diphosphatidylglycerol. In addition, two unidentified phospholipids and four unidentified glycolipids were detected in strain KRD168^T, whilst strain KRD185^T also contained four unidentified phospholipids, two unidentified glycolipids and an unidentified glycophospholipid. Moreover, some chemotaxonomic characteristics, such as the metabolic profile and the cellular fatty acid composition, differentiated strains KRD168^T and KRD185^T from *P. petroleophila* DSM 43193^T and *P. broussonetiae* Gen 01^T, respectively. In particular, strain KRD168^T was negative for α-galactosidase and α-glucosidase activity, while *P. petroleophila* DSM 43193^T was positive. Similarly, strain KRD185^T was positive for α-glucosidase activity, while *P. broussonetiae* Gen 01^T reported no activity. Furthermore, the relatively low proportion of *iso*-branched pentadecanoic acid (11.0% vs 25.2%) and the relatively high proportion of *iso*-branched tetradecanoic acid (7.6% vs 2.0%) distinguished strain KRD168^T from *P. petroleophila* DSM 43193^T. Likewise, the relatively low proportion of *iso*-branched tetradecanoic acid (1.9 % vs 5.6 %) and hexadecanoic acid (3.6 % vs 9.8 %), as well as the relatively high proportion of *iso*-branched pentadecanoic acid (7.7 % vs 2.1 %) differentiated strain KRD185^{T}from *P. broussonetiae* Gen 01^{T,T}.

Strains KRD168^T, KRD185^T and *P. petroleophila* DSM 43193^T were cultured on ISP2 agar for 28 days using an inclined coverslip, and their morphology was observed using a Nikon Eclipse TE2000-S Inverted microscope fitted with a 100×/1.3 numerical aperture objective lens (Nikon). Illumination was sourced from a mercury arc lamp with appropriate emission filters for FITC/PI imaging. Fluorescence microscopy was carried out using fluorescein-conjugated wheat germ agglutinin (FITC-WGA) and propidium iodide (PI) to describe structures in the aerial hyphae and apical tip growth [51]. Phase-contrast and fluorescence images were acquired sequentially using an ORCA-100 CCD camera (Hamamatsu).

Table 1. Differential phenotypic characteristics of the analysed strains

Strains: 1, *Pseudonocardia abyssalis* sp. nov. KRD168^T; 2, *Pseudonocardia oceani* sp. nov. KRD185^T; 3, *Pseudonocardia petroleophila* DSM 43193^T (from Zhao *et al.* [53]); 4, *Pseudonocardia hydrocarbonoxydans* DSM 43281^T (from Zhang *et al.* [15]); 5, *Pseudonocardia broussonetiae* Gen 01^T (from Mo *et al.* [54]).

	1	2	3	4	5
Morphology on:					
ISP2	Yellow	Orange	Yellow	Yellow	Yellow
ISP5	White	Yellow	White	White	Yellow
Growth at:					
NaCl (%)	0–3	0–3	0–4	0–2	0–8
pH	6–10	6–10	6–10	6–9	5–8
API ZYM					
Alkaline phosphatase	+	+	+	+	−
Esterase (C4)	+	+	+	−	+
Cystine arylamidase	−	+	+	+	−
Trypsin	−	−	+	+	−
α-Chymotrypsin	−	−	+	+	−
Naphthol-AS-BI-phosphohydrolase	+	+	−	+	+
α-Galactosidase	−	−	+	+	−
β-Galactosidase	+	−	+	+	−
α-Glucosidase	−	+	+	+	−
Fatty acids (>1%)					
$C_{12:0}$	ND	ND	ND	ND	1.2
$C_{14:0}$	ND	ND	ND	ND	2.9
iso-$C_{14:0}$	7.6	1.9	2.0	1.5	5.6
$C_{15:1}\omega 6c$	ND	ND	ND	1.9	2.6
iso-$C_{15:0}$	11.0	7.7	25.2	17.9	2.1
iso-$C_{16:1}$ H	3.2	8.9	2.6	5.8	10.7
iso-$C_{16:0}$	36.3	38.5	43.2	31.7	36.1
$C_{16:1}$ 2-OH	ND	ND	2.4	ND	ND
$C_{16:0}$	4.7	3.6	2.0	3.6	9.8
iso-$C_{17:0}$	4.2	2.0	10.2	3.2	ND
anteiso-$C_{17:0}$	1.1	2.4	ND	1.4	ND
$C_{17:1}\omega 8c$	8.0	5.1	ND	8.3	4.0
$C_{17:0}$	3.4	1.6	ND	1.7	1.4
$C_{17:0}$ 10 methyl	2.4	2.7	1.5	1.9	ND
$C_{18:1}\omega 9c$	1.2	ND	ND	ND	ND

ND, Not detected.

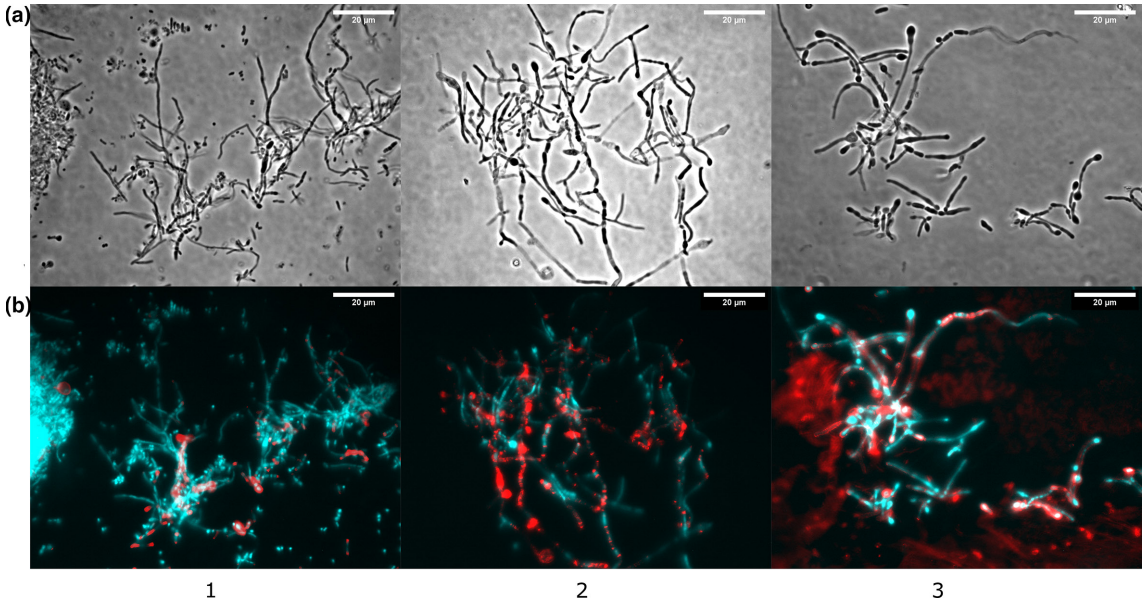

Fig. 3. (a) Phase contrast and (b) widefield epifluorescence microscopy of: 1, *Pseudonocardia abyssalis* sp. nov. KRD168^T; 2, *Pseudonocardia oceani* sp. nov. KRD185^T; and 3, *Pseudonocardia petroleophila* DSM 43193^T; growth on ISP2 for 28 days. Fluorescence microscopy of DNA (cyan) and nascent peptidoglycan (red) is shown. Bar, 20 µm.

Image processing and analysis was performed using FIJI [52]. Budding substrate and aerial hyphae with swelling and side branches were observed (Fig. 3). A more filamentous structure was observed for strain KRD185^T than for strain KRD168^T. Spores were rod-like, mostly 0.6–1.4 µm wide and 1.2–1.9 µm long for strain KRD168^T, and 0.7–1.6 µm wide and 1.4–3.9 µm long for strain KRD185^T. Active growth and sporulation were still observed after 28 days.

Based on the phenotypic and chemotaxonomic analysis, strains KRD168^T and KRD185^T exhibit characteristic markers for the genus *Pseudonodardia*. Furthermore, the phenotypic characterization and genomic relatedness of strains KRD168^T and KRD185^T differentiate them from their closest phylogenetic neighbours. In conclusion, we suggest that the two strains represent two novel species, for which the names *Pseudonocardia abyssalis* sp. nov. and *Pseudonocardia oceani* sp. nov. are proposed.

DESCRIPTION OF *PSEUDONOCARDIA ABYSSALIS* SP. NOV.

Pseudonocardia abyssalis (a.bys.sa'lis. L. fem. n. *abyssus* an abyss, deep sea; L. fem. suff. -*alis* suffix denoting pertaining to; N.L. fem. adj. *abyssalis* pertaining to the abyssal depths of the ocean).

Aerobic, Gram-positive, non-motile actinomycetes. Forms yellow aerial and substrate mycelia on ISP2, while white substrate and aerial mycelia are produced on ISP3, ISP4 and ISP5. Growth occurs at 20–30 °C, at pH 6–10 and in the presence of 0–3% (w/v) NaCl. Substrate mycelium is fragmented and rod-shaped spore chains are formed on aerial hyphae and substrate mycelium. The following enzymatic reactions are positive: urease, acetoin production, gelatine hydrolysis, alkaline phosphatase, esterase, esterase lipase, leucine arylamidase and valine arylamidase. The major menaquinone is MK-8(H_4) (91.5%), while MK-8(H_6) (8.5%) is also present. The cell wall contains *meso*-diaminopimelic acid as the diagnostic amino acid, and the major whole-cell sugar is glucose with minor amounts of arabinose and xylose. The polar lipid profile includes phosphatidylethanolamine and diphosphatidylglycerol. The predominant fatty acid is iso-$C_{16:0}$, while iso-$C_{15:0}$, $C_{17:1}\omega 8c$ and iso-$C_{14:0}$ are also major components.

The type strain, KRD168^T (=DSM 111918^T =NCIMB 15270^T), was isolated from sediments collected from the Southern Ocean at a depth of 4539 m. The genome of the type strain is characterized by a size of 6.31 Mbp and a G+C content of 73.44 mol%.

DESCRIPTION OF *PSEUDONOCARDIA OCEANI* SP. NOV.

Pseudonocardia oceani (o.ce.a'ni. L. gen. n. *oceani* of the ocean).

Aerobic, Gram-positive, non-motile actinomycetes. Forms yellow substrate mycelium and orange aerial mycelium with white spores formed from the aerial hyphae on ISP2. On ISP3, ISP4 and ISP5 white substrate and aerial mycelia are produced. Growth occurs at 20–30 °C, at pH 6–10 and in the presence of 0–3% (w/v) NaCl. Substrate mycelium is fragmented and rod-shaped spore chains are formed on aerial hyphae and substrate mycelium. The following enzymatic reactions are positive: alkaline phosphatase, esterase,

esterase lipase, leucine arylamidase, valine arylamidase, cystine arylamidase, acid phosphatase, naphthol-AS-BI-phosphohydrolase, α-glucosidase and β-glucosidase The major menaquinone is MK-8(H_4) (96.2%), while MK-8(H_2) (2.9%) and MK-8(H_6) (1.5%) are also present. The cell wall contains *meso*-diaminopimelic acid as the diagnostic amino acid, and the major whole-cell sugar is glucose with minor amounts of arabinose and xylose. The polar lipid profile includes phosphatidylethanolamine and diphosphatidylglycerol. The predominant fatty acid is iso-$C_{16:0}$, while iso-$C_{16:1}$ H, iso-$C_{15:0}$ and $C_{17:1}$ω8c are also major components.

The type strain, KRD185^T (=DSM 111919^T=NCIMB 15269^T), was isolated from sediments collected from the Southern Ocean at a depth of 4060 m. The genome of the type strain is characterized by a size of 6.82 Mbp and a G+C content of 73.98 mol%.

Funding information
J.P. is supported by Programa de Innovación y Capital Humano para la Competitividad (PINN) of The Ministry of Science, Technology and Telecommunications of Costa Rica (MICITT) grant 2-1-4-17-1-037.

Conflicts of interest
The authors declare that there are no conflicts of interest.

References

1. Henssen A. Beiträge zur Morphologie und Systematik der thermophilen Actinomyceten [Contributions to the morphology and systematics of the thermophilic actinomycetes]. *Archiv Mikrobiol* 1957;26:373–414.
2. Reichert K, Lipski A, Pradella S, Stackebrandt E, Altendorf K. *Pseudonocardia asaccharolytica* sp. nov. and *Pseudonocardia sulfidoxydans* sp. nov., two new dimethyl disulfide-degrading actinomycetes and emended description of the genus *Pseudonocardia*. *Int J Syst Bacteriol* 1998;48 Pt 2:441–449.
3. Warwick S, Bowen T, McVeigh H, Embley TM. A phylogenetic analysis of the family *Pseudonocardiaceae* and the genera *Actinokineospora* and *Saccharothrix* with 16S rRNA sequences and a proposal to combine the genera *Amycolata* and *Pseudonocardia* in an emended genus *Pseudonocardia*. *Int J Syst Bacteriol* 1994;44:293–299.
4. Huang Y, Wang L, Lu Z, Hong L, Liu Z, *et al*. Proposal to combine the genera *Actinobispora* and *Pseudonocardia* in an emended genus *Pseudonocardia*, and description of *Pseudonocardia zijingensis* sp. nov.. *Int J Syst Evol Microbiol* 2002;52:977–982.
5. Park SW, Park ST, Lee JE, Kim YM. *Pseudonocardia carboxydivorans* sp. nov., a carbon monoxide-oxidizing actinomycete, and an emended description of the genus *Pseudonocardia*. *Int J Syst Evol Microbiol* 2008;58:2475–2478.
6. Huang Y, Goodfellow M. Pseudonocardia. Trujillo ME, Dedysh S, DeVos P, Hedlund B and Kämpfer P (eds). In: *Bergey's Manual of Systematics of archaea and bacteria*. Wiley; 2015. pp. 1–32.
7. Parte AC, Sardà Carbasse J, Meier-Kolthoff JP, Reimer LC, Göker M. List of prokaryotic names with standing in nomenclature (LPSN) moves to the DSMZ. *Int J Syst Evol Microbiol* 2020;70:5607–5612.
8. LPSN - List of Prokaryotic names with Standing in Nomenclature. Genus *Pseudonocardia*. . https://lpsn.dsmz.de/genus/pseudonocardia
9. Gontang EA, Fenical W, Jensen PR. Phylogenetic diversity of gram-positive bacteria cultured from marine sediments. *Appl Environ Microbiol* 2007;73:3272–3282.
10. Maldonado LA, Stach JEM, Pathom-aree W, Ward AC, Bull AT, *et al*. Diversity of cultivable actinobacteria in geographically widespread marine sediments. *Antonie van Leeuwenhoek* 2005;87:11–18.
11. Chanama S, Janphen S, Suriyachadkun C, Chanama M. *Pseudonocardia mangrovi* sp. nov., isolated from soil. *Int J Syst Evol Microbiol* 2018;68:2949–2955.
12. Liu Z-P, Wu J-F, Liu Z-H, Liu S-J. *Pseudonocardia ammonioxydans* sp. nov., isolated from coastal sediment. *Int J Syst Evol Microbiol* 2006;56:555–558.
13. Zhang D-F, Jiang Z, Li L, Liu B-B, Zhang X-M, *et al*. *Pseudonocardia sediminis* sp. nov., isolated from marine sediment. *Int J Syst Evol Microbiol* 2014;64:745–750.
14. Tian X-P, Long L-J, Li S-M, Zhang J, Xu Y, *et al*. *Pseudonocardia antitumoralis* sp. nov., a deoxynyboquinone-producing actinomycete isolated from a deep-sea sediment. *Int J Syst Evol Microbiol* 2013;63:893–899.
15. Zhang G, Wang L, Li J, Zhou Y. *Pseudonocardia profundimaris* sp. nov., isolated from marine sediment. *Int J Syst Evol Microbiol* 2017;67:1693–1697.
16. Millán-Aguiñaga N, Soldatou S, Brozio S, Munnoch JT, Howe J, *et al*. Awakening ancient polar Actinobacteria: diversity, evolution and specialized metabolite potential. *Microbiol* 2019;165:1169–1180.
17. Soldatou S, Eldjárn GH, Ramsay A, van der Hooft JJJ, Hughes AH, *et al*. Comparative metabologenomics analysis of polar actinomycetes. *Mar Drugs* 2021;19:103.
18. Howe JA, Shimmield TM, Diaz R. Deep-water sedimentary environments of the Northwestern Weddell Sea and South Sandwich Islands, Antarctica. *Deep Res Part II Top Stud Oceanogr* 2004;51:1489–1514.
19. Mincer TJ, Jensen PR, Kauffman CA, Fenical W. Widespread and persistent populations of a major new marine actinomycete taxon in ocean sediments. *Appl Environ Microbiol* 2002;68:5005–5011.
20. Shirling ET, Gottlieb D. Methods for characterization of *Streptomyces* species. *Int J Syst Bacteriol* 1966;16:313–340.
21. Weisburg WG, Barns SM, Pelletier DA, Lane DJ. 16S ribosomal DNA amplification for phylogenetic study. *J Bacteriol* 1991;173:697–703.
22. Altschul SF, Gish W, Miller W, Myers EW, Lipman DJ. Basic local alignment search tool. *J Mol Biol* 1990;215:403–410.
23. Yoon S-H, Ha S-M, Kwon S, Lim J, Kim Y, *et al*. Introducing Ezbiocloud: A taxonomically united database of 16s rrna gene sequences and whole-genome assemblies. *Int J Syst Evol Microbiol* 2017;67:1613–1617.
24. Larkin MA, Blackshields G, Brown NP, Chenna R, McGettigan PA, *et al*. Clustal W and clustal x version 2.0. *Bioinformatics* 2007;23:2947–2948.
25. Saitou N, Nei M. The neighbor-joining method: a new method for reconstructing phylogenetic trees. *Mol Biol Evol* 1987;4:406–425.
26. Tamura K, Nei M. Estimation of the number of nucleotide substitutions in the control region of mitochondrial DNA in humans and chimpanzees. *Mol Biol Evol* 1993;10:512–526.
27. Kumar S, Stecher G, Li M, Knyaz C, Tamura K. MEGA X: Molecular evolutionary genetics analysis across computing platforms. *Mol Biol Evol* 2018;35:1547–1549.
28. Felsenstein J. Confidence limits on phylogenies: an approach using the bootstrap. *Evolution* 1985;39:783–791.
29. Marmur J. A procedure for the isolation of deoxyribonucleic acid from micro-organisms. *J Mol Biol* 1961;3:208–218.
30. Kolmogorov M, Yuan J, Lin Y, Pevzner PA. Assembly of long, error-prone reads using repeat graphs. *Nat Biotechnol* 2019;37:540–546.
31. Langmead B, Salzberg SL. Fast gapped-read alignment with Bowtie 2. *Nat Methods* 2012;9:357–359.
32. Walker BJ, Abeel T, Shea T, Priest M, Abouelliel A, *et al*. Pilon: an integrated tool for comprehensive microbial variant detection and genome assembly improvement. *PLoS One* 2014;9:e112963.
33. Chin C-S, Alexander DH, Marks P, Klammer AA, Drake J, *et al*. Nonhybrid, finished microbial genome assemblies from long-read SMRT sequencing data. *Nat Methods* 2013;10:563–569.
34. Koren S, Walenz BP, Berlin K, Miller JR, Bergman NH, *et al*. Canu: scalable and accurate long-read assembly via adaptive k-mer weighting and repeat separation. *Genome Res* 2017;27:722–736.

35. Vaser R, Šikić M. Raven: A *de novo* genome assembler for long reads. *bioRxiv* 2020:08.07.242461.
36. Wick RR, Judd LM, Gorrie CL, Holt KE. Unicycler: Resolving bacterial genome assemblies from short and long sequencing reads. *PLoS Comput Biol* 2017;13:1–22.
37. Bankevich A, Nurk S, Antipov D, Gurevich AA, Dvorkin M, *et al*. SPAdes: A new genome assembly algorithm and its applications to single-cell sequencing. *J Comput Biol* 2012;19:455–477.
38. Gurevich A, Saveliev V, Vyahhi N, Tesler G. QUAST: Quality assessment tool for genome assemblies. *Bioinformatics* 2013;29:1072–1075.
39. Simão FA, Waterhouse RM, Ioannidis P, Kriventseva EV, Zdobnov EM. BUSCO: Assessing genome assembly and annotation completeness with single-copy orthologs. *Bioinformatics* 2015;31:3210–3212.
40. Meier-Kolthoff JP, Auch AF, Klenk H-P, Göker M. Genome sequence-based species delimitation with confidence intervals and improved distance functions. *BMC Bioinformatics* 2013;14:60.
41. Jain C, Rodriguez-R LM, Phillippy AM, Konstantinidis KT, Aluru S. High throughput ANI analysis of 90K prokaryotic genomes reveals clear species boundaries. *Nat Commun* 2018;9:1–8.
42. Richter M, Rosselló-Móra R. Shifting the genomic gold standard for the prokaryotic species definition. *Proc Natl Acad Sci U S A* 2009;106:19126–19131.
43. Meier-Kolthoff JP, Klenk H-P, Göker M. Taxonomic use of DNA G+C content and DNA-DNA hybridization in the genomic age. *Int J Syst Evol Microbiol* 2014;64:352–356.
44. Alanjary M, Steinke K, Ziemert N. AutoMLST: an automated web server for generating multi-locus species trees highlighting natural product potential. *Nucleic Acids Res* 2019;47:276–282.
45. Nolof G, Hirsch P. *Nocardia hydrocarbonoxydans* n. spec., ein oligocarbophiler Actinomycet. *Arch Mikrobiol* 1962;44:266–277.
46. Kuykendall LD, Roy MA, O'Neill JJ, Devine TE. Fatty acids, antibiotic resistance, and deoxyribonucleic acid homology groups of Bradyrhizobium japonicum. *Int J Syst Bacteriol* 1988;38:358–361.
47. Miller LT. Single derivatization method for routine analysis of bacterial whole-cell fatty acid methyl esters, including hydroxy acids. *J Clin Microbiol* 1982;16:584–586.
48. Tindall BJ, Sikorski J, Smibert RA, Krieg NR. Phenotypic characterization and the principles of comparative systematics. In: *Methods for General and Molecular Microbiology*. Washington, DC, USA: ASM Press, 2014. pp. 330–393.
49. Rhuland LE, Work E, Denman RF, Hoare DS. The behavior of the isomers of α,ε-diaminopimelic acid on paper chromatograms. *J Am Chem Soc* 1955;77:4844–4846.
50. Staneck JL, Roberts GD. Simplified approach to identification of aerobic actinomycetes by thin-layer chromatography. *Appl Microbiol* 1974;28:226–231.
51. Schwedock J, McCormick JR, Angert ER, Nodwell JR, Losick R. Assembly of the cell division protein FtsZ into ladder-like structures in the aerial hyphae of *Streptomyces coelicolor*. *Mol Microbiol* 1997;25:847–858.
52. Schindelin J, Arganda-Carreras I, Frise E, Kaynig V, Longair M, *et al*. Fiji: An open-source platform for biological-image analysis. *Nat Methods* 2012;9:676–682.
53. Zhao GZ, Zhu WY, Li J, Xie Q, Xu LH, *et al*. *Pseudonocardia serianimatus* sp. nov., a novel actinomycete isolated from the surface-sterilized leaves of *Artemisia annua* L. *Antonie van Leeuwenhoek* 2011;100:521–528.
54. Mo P, Zhao Y, Liu J, Xu Z, Gao J. *Pseudonocardia broussonetiae* sp. nov., an endophytic actinomycete isolated from the roots of Broussonetia papyrifera. *Int J Syst Evol Microbiol* 2021;71:004680.

Supplementary material

Pseudonocardia abyssalis sp. nov. and *Pseudonocardia oceani* sp. nov., two novel actinomycetes isolated from the deep Southern Ocean

Jonathan Parra[1], Sylvia Soldatou[1, 2], Liam M. Rooney[1, 3], Katherine R. Duncan[1*]

[1]Strathclyde Institute of Pharmacy and Biomedical Sciences, University of Strathclyde, Glasgow G4 0RE, UK

[2]Present address: School of Pharmacy and Life Sciences, Robert Gordon University, Aberdeen AB10 7GJ, UK

[3]Present address: Institute of Biological Chemistry, Biophysics and Bioengineering, School of Engineering and Physical Sciences, Heriot-Watt University, Edinburgh EH14 4AS, UK

Correspondence

Katherine R. Duncan

Email: katherine.duncan@strath.ac.uk

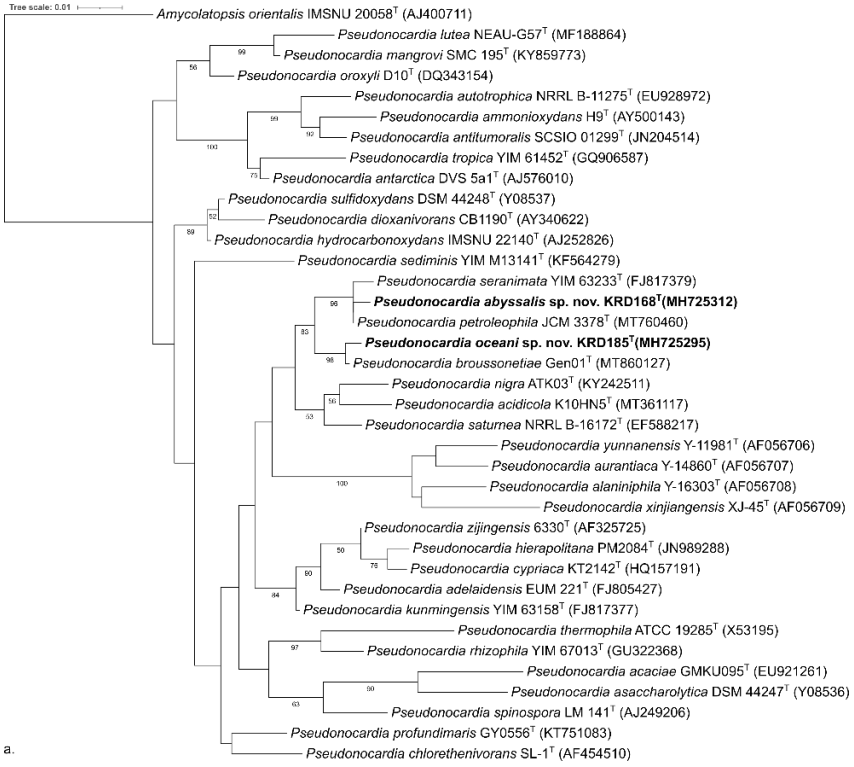

a.

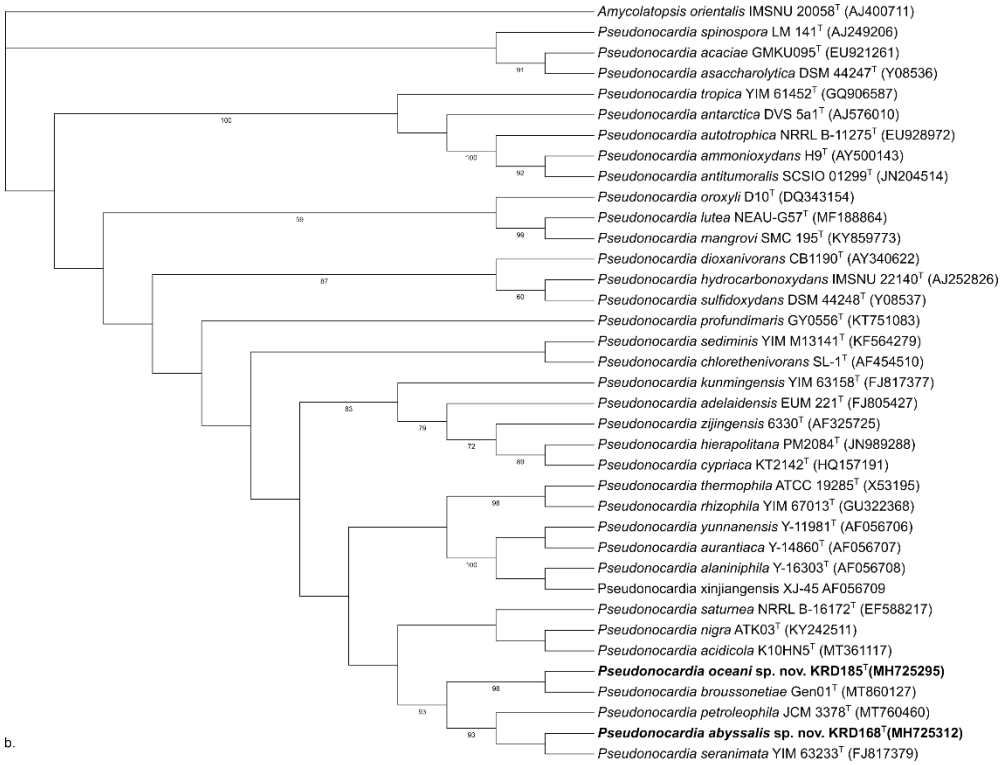

Fig. S1. Bootstrap consensus tree inferred from 1000 replicates. Branches corresponding to partitions reproduced in less than 50% bootstrap replicates are collapsed. The evolutionary history was inferred using the Maximum Likelihood (a), and Maximum Parsimony (b).

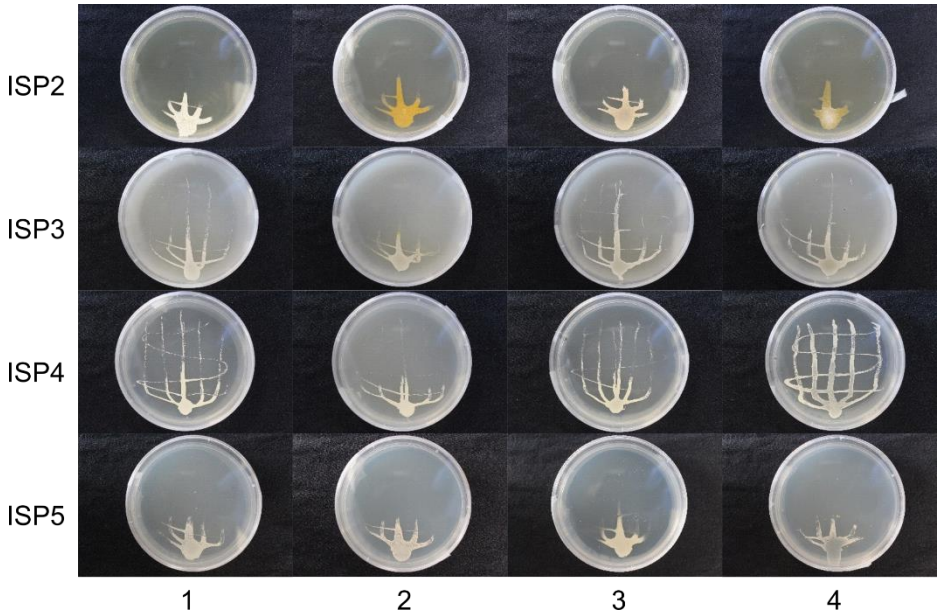

Fig. S2. Strain morphology on analysed media: 1, *Pseudonocardia abyssalis* sp. nov. KRD168^T; 2, *Pseudonocardia oceani* sp. nov. KRD185^T; 3, *Pseudonocardia petroleophila* DSM 43193^T; and 4, *Pseudonocardia hydrocarbonoxydans* DSM 43281^T.

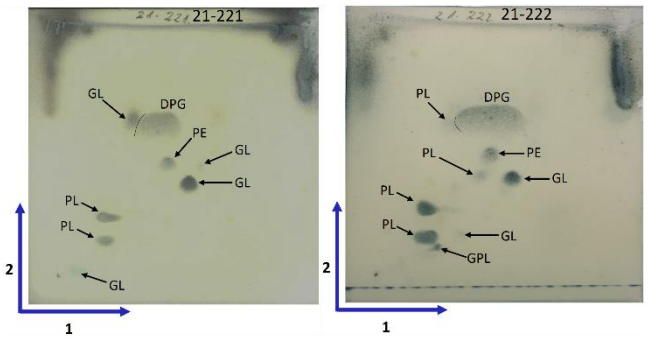

Fig. S3. Polar lipid profile of 1, *Pseudonocardia abyssalis* sp. nov. KRD168^T; and 2, *Pseudonocardia oceani* sp. nov. KRD185^T; after two-dimensional thin-layer chromatography (TLC). PE, phosphatidylethanolamine; DPG, diphosphatidylglycerol; PL, unidentified phospholipid; GL, unidentified glycolipid; GPL, unidentified glycophospholipid.

Table S1. Contiguity and quality evaluation of genome assemblies of *Pseudonocardia abyssalis* sp. nov. KRD168^T and *Pseudonocardia oceani* sp. nov. KRD185^T.

	Coverage	Contigs	Largest contig (bp)	Length (bp)	N50 (bp)	BUSCO (% complete single-copy genes)
KRD168^T	1150.6x PacBio 215.7x Illumina	2	6273229	6305989	6273229	100
KRD185^T	217.1 PacBio 29.6x Illumina	3	6661555	6821805	6661555	100

Table S2. Overview of the whole-genome sequences of *Pseudonocardia* spp. used in this study for the genomic analysis.

Organism Name	Strain	Assembly	Level	Size (Mb)	GC%	Replicons	WGS
Pseudonocardia petroleophila	CGMCC 4.1532	GCA_014235185.1	Complete	6.49014	74.0	chromosome:NZ_CP060131.1/CP060131.1	-
Pseudonocardia broussonetiae	Gen 01	GCA_013155125.1	Complete	7.28743	74.4	chromosome: NZ_CP053564.1/CP053564.1 plasmid unnamed1: NZ_CP053565.1/CP053565.1 plasmid unnamed2: NZ_CP053566.1/CP053566.1 plasmid unnamed3: NZ_CP053567.1/CP053567.1	-
Pseudonocardia hydrocarbonoxydans	NBRC 14498	GCA_006539565.1	Contig	5.29005	74.5	-	BJNG01
Pseudonocardia sp.	CNS-139	GCA_001942415.1	Scaffold	7.12539	74.2	-	MKJX01
Pseudonocardia sp.	MH-G8	GCA_002262885.1	Scaffold	10.1794	72.6	-	NKYF01
Pseudonocardia thermophila	DSM 43832	GCA_900142365.1	Contig	6.09821	72.9	-	FRAP01
Pseudonocardia ammonioxydans	CGMCC 4.1877	GCA_900115005.1	Scaffold	7.36151	73.5	-	FOUY01
Pseudonocardia autotrophica	DSM 535	GCA_004361965.1	Contig	7.57033	72.8	-	SNWB01
Pseudonocardia sp.	AL041005-10	GCA_001294605.1	Complete	6.14334	74.4	chromosome:NZ_CP011862.1/CP011862.1	-
Pseudonocardia oroxyli	CGMCC 4.3143	GCA_900102195.1	Scaffold	6.11157	73.0	-	FNBE01
Pseudonocardia dioxanivorans	CB1190	GCA_000196675.1	Complete	7.30399	73.2	chromosome:NC_015312.1/CP002593.1; plasmid pPSED01:NC_015314.1/CP002594.1; plasmid pPSED03:NC_015313.1/CP002598.1	-
Pseudonocardia asaccharolytica	DSM 44247	GCA_000423625.1	Scaffold	5.05684	71.8	-	AUII01
Pseudonocardia acaciae	DSM 45401	GCA_000620785.1	Scaffold	9.93133	72.3	-	JIAI01
Pseudonocardia spinosispora	DSM 44797	GCA_000429025.1	Scaffold	9.53756	69.4	-	AUBB01
Amycolatopsis orientalis	KCTC 9412	GCA_000478275.1	Contig	9.06245	69.0	-	ASJB01

Table S3. List of orthologous genes with confirmed conserved functions used to construct the multi-locus tree.

Accession number	Gene	Name
TIGR00133	gatB	aspartyl/glutamyl-tRNA(Asn/Gln) amidotransferase, B subunit
TIGR01798	cit_synth_I	citrate (Si)-synthase
TIGR00135	gatC	aspartyl/glutamyl-tRNA(Asn/Gln) amidotransferase, C subunit
TIGR00138	rsmG_gidB	16S rRNA (guanine(527)-N(7))-methyltransferase RsmG
TIGR00033	aroC	chorismate synthase
TIGR00031	UDP-GALP_mutase	UDP-galactopyranose mutase
TIGR00036	dapB	4-hydroxy-tetrahydrodipicolinate reductase
TIGR00234	tyrS	tyrosine--tRNA ligase
TIGR01203	HGPRTase	hypoxanthine phosphoribosyltransferase
TIGR00331	hrcA	heat-inducible transcription repressor HrcA
TIGR01044	rplV_bact	ribosomal protein uL22
TIGR00652	DapF	diaminopimelate epimerase
TIGR00338	serB	phosphoserine phosphatase SerB
TIGR01327	PGDH	phosphoglycerate dehydrogenase
TIGR01146	ATPsyn_F1gamma	ATP synthase F1, gamma subunit
TIGR01280	xseB	exodeoxyribonuclease VII, small subunit
TIGR01966	RNasePH	ribonuclease PH
TIGR00521	coaBC_dfp	phosphopantothenoylcysteine decarboxylase / phosphopantothenate--cysteine ligase
TIGR03594	GTPase_EngA	ribosome-associated GTPase EngA
TIGR00088	trmD	tRNA (guanine(37)-N(1))-methyltransferase
TIGR00855	L12	ribosomal protein bL12
TIGR00083	ribF	riboflavin biosynthesis protein RibF
TIGR00244	TIGR00244	transcriptional regulator NrdR
TIGR01039	atpD	ATP synthase F1, beta subunit
TIGR01134	purF	amidophosphoribosyltransferase
TIGR00086	smpB	SsrA-binding protein
TIGR01030	rpmH_bact	ribosomal protein bL34
TIGR00690	rpoZ	DNA-directed RNA polymerase, omega subunit
TIGR01032	rplT_bact	ribosomal protein bL20
TIGR00019	prfA	peptide chain release factor 1
TIGR00396	leuS_bact	leucine--tRNA ligase
TIGR00012	L29	ribosomal protein uL29
TIGR01978	sufC	FeS assembly ATPase SufC
TIGR00150	T6A_YjeE	tRNA threonylcarbamoyl adenosine modification protein YjeE
TIGR00152	TIGR00152	dephospho-CoA kinase
TIGR00154	ispE	4-(cytidine 5'-diphospho)-2-C-methyl-D-erythritol kinase
TIGR00313	cobQ	cobyric acid synthase CobQ
TIGR00981	rpsL_bact	ribosomal protein uS12
TIGR00090	rsfS_iojap_ybeB	ribosome silencing factor
TIGR00959	ffh	signal recognition particle protein
TIGR01308	rpmD_bact	ribosomal protein uL30
TIGR01302	IMP_dehydrog	inosine-5'-monophosphate dehydrogenase
TIGR01029	rpsG_bact	ribosomal protein uS7

TIGR01021	rpsE_bact	ribosomal protein uS5
TIGR01024	rplS_bact	ribosomal protein bL19
TIGR00382	clpX	ATP-dependent Clp protease, ATP-binding subunit ClpX
TIGR00061	L21	ribosomal protein bL21
TIGR00639	PurN	phosphoribosylglycinamide formyltransferase
TIGR01410	tatB	twin arginine-targeting protein translocase TatB
TIGR00635	ruvB	Holliday junction DNA helicase RuvB
TIGR00581	moaC	molybdenum cofactor biosynthesis protein C
TIGR01011	rpsB_bact	ribosomal protein uS2
TIGR01850	argC	N-acetyl-gamma-glutamyl-phosphate reductase
TIGR00577	fpg	DNA-formamidopyrimidine glycosylase
TIGR01169	rplA_bact	ribosomal protein uL1
TIGR00928	purB	adenylosuccinate lyase
TIGR00482	TIGR00482	nicotinate (nicotinamide) nucleotide adenylyltransferase
TIGR00962	atpA	ATP synthase F1, alpha subunit
TIGR00922	nusG	transcription termination/antitermination factor NusG
TIGR01164	rplP_bact	ribosomal protein uL16
TIGR01009	rpsC_bact	ribosomal protein uS3
TIGR00168	infC	translation initiation factor IF-3
TIGR02012	tigrfam_recA	protein RecA
TIGR00281	TIGR00281	segregation and condensation protein B
TIGR00166	S6	ribosomal protein bS6
TIGR00414	serS	serine--tRNA ligase
TIGR02422	protocat_beta	protocatechuate 3,4-dioxygenase, beta subunit
TIGR00560	pgsA	CDP-diacylglycerol--glycerol-3-phosphate 3-phosphatidyltransferase
TIGR00419	tim	triose-phosphate isomerase
TIGR01171	rplB_bact	ribosomal protein uL2
TIGR00810	secG	preprotein translocase, SecG subunit
TIGR00952	S15_bact	ribosomal protein uS15
TIGR00119	acolac_sm	acetolactate synthase, small subunit
TIGR00114	lumazine-synth	6,7-dimethyl-8-ribityllumazine synthase
TIGR00116	tsf	translation elongation factor Ts
TIGR00059	L17	ribosomal protein bL17
TIGR00708	cobA	cob(I)yrinic acid a,c-diamide adenosyltransferase
TIGR01464	hemE	uroporphyrinogen decarboxylase
TIGR00468	pheS	phenylalanine--tRNA ligase, alpha subunit
TIGR01737	FGAM_synth_I	phosphoribosylformylglycinamidine synthase I
TIGR01066	rplM_bact	ribosomal protein uL13
TIGR02727	MTHFS_bact	5-formyltetrahydrofolate cyclo-ligase
TIGR02729	Obg_CgtA	Obg family GTPase CgtA
TIGR00020	prfB	peptide chain release factor 2
TIGR00228	ruvC	crossover junction endodeoxyribonuclease RuvC
TIGR00670	asp_carb_tr	aspartate carbamoyltransferase
TIGR00029	S20	ribosomal protein bS20
TIGR03263	guanyl_kin	guanylate kinase
TIGR03635	uS17_bact	ribosomal protein uS17

TIGR00184	purA	adenylosuccinate synthase
TIGR03632	uS11_bact	ribosomal protein uS11
TIGR01051	topA_bact	DNA topoisomerase I
TIGR01358	DAHP_synth_II	3-deoxy-7-phosphoheptulonate synthase

Table S4. Buffers composition used in the modified media for the pH tolerance assay.

pH	Component	Molarity (mol/L)
4	Sodium citrate dihydrate	0.0335
	Citric acid	0.0665
5	Sodium citrate dihydrate	0.0577
	Citric acid	0.0423
6	K_2HPO_4	0.0138
	KH_2PO_4	0.0862
7	K_2HPO_4	0.0536
	KH_2PO_4	0.0464
8	K_2HPO_4	0.0935
	KH_2PO_4	0.0065
9.2	Sodium bicarbonate	0.0910
	Sodium carbonate	0.0090
10	Sodium bicarbonate	0.0461
	Sodium carbonate	0.0539